SUPPLEMENTAL MATERIAL

Supplementary Materials and Methods

Strains, Plasmids and Cell growth

All *Brucella* strains used in this study (Table S1) were derived from *B. abortus* 544 Nal^R (spontaneous nalidixic acid-resistant mutant), and were routinely cultivated in Tryptic Soy Broth (TSB). *C. crescentus* CB15N was grown in peptone-yeast extract (PYE medium). *S. meliloti* 1021 was grown in Luria Bertani (LB). The *E. coli* strains deriving from MG1655, DH10B (Invitrogen Life-Technologies), DB3.1 (Invitrogen Life-Technologies), BL21(DE3) (Novagen), S17-1 (21), DH5α (Bethesda Research Laboratories) and MT616 (10) were cultivated in LB broth. Antibiotics were used at the following concentrations when appropriate: nalidixic acid, 25 µg ml^{-1}; kanamycin, 20 µg ml^{-1}; chloramphenicol, 20 µg ml^{-1}; ampicillin, 100 µg ml^{-1}; gentamicin, 50 µg ml^{-1}; nourseothricine, 25 µg ml^{-1}. Plasmids (Table S1) were mobilized from *E. coli* strain S17-1 into *B. abortus* and *C. crescentus* by bacterial conjugation (8), and from *E. coli* strain DH5α into *S. meliloti* by triparental mating as described previously (12). Induction of gene expression under P_{xylX} and P_{lac} was achieved with 0.3% xylose and 1 mM IPTG respectively. In corresponding control experiments, media were supplemented with 0.2% glucose (PYEG) instead of xylose (PYEX). The growth media and yeast genetic techniques have been described previously (20). Full details about the Y2H assays are available in the Supplemental material.

Molecular Techniques

Allelic replacement

B. abortus 544 knock-out and XDB1155 (*pdhS-cfp*) mutants were obtained by allelic replacement. Briefly, for generating *B. abortus* Δ*fumC* (XDB1157) and Δ*fumA* (XDB1160) mutant strains, upstream and downstream regions flanking *fumC* and *fumA* genes were amplified by PCR using the following primer pairs: (*i*) *fumC*up1 and *fumC*up2; (*ii*) *fumC*down1 and *fumC*down2; (*i*) *fumA*up1 and *fumA*up2; (*ii*) *fumA*down1 and *fumA*down2. A second PCR using *fumC*up1 and *fumC*down2 primers or *fumA*up1 and *fumA*down2 primers allowed us to associate the PCR products. The final PCR products were cloned in pGEM-T Easy (Promega) to generate pGEM-T-Δ*fumC* and pGEM-T-Δ*fumA*, respectively. Finally, the Δ*fumC* and Δ*fumA* fragments were excised from pGEM-T-Δ*fumC* and pGEM-T-Δ*fumA* by *Not*I restriction and subsequently cloned into *Not*I-cut pJQ200-uc1 (Donnenberg and Kaper, 1991) to generate pJM056 and pJM082, respectively.

Concerning *pdhS-cfp*, allelic replacement was performed as follows : upstream and downstream regions just flanking the stop codon of *pdhS* coding sequence were amplified by PCR using the following primer pairs: (*i*) *pdhS-cfp*up1 and *pdhS-cfp*up2; (*ii*) *pdhS-cfp*down1 and *pdhS-cfp*down2. A second PCR using *pdhS-cfp*up1 and *pdhS-cfp*down2 primers allowed us to associate the PCR products. The final PCR products were cloned into pGEM-T Easy (Promega) to generate pGEM-T-*pdhS'C*. In parallel, *cfp* was amplified by PCR on the pFA6-*cfp-nat*MX6 (22) with *cfp*up and *cfp*down primers and inserted at the unique *Eco*RV site pGEM-T-*pdhS'C* plasmid to generate the pGEM-T-*pdhS'C-cfp*. Finally, the *pdhS'N-cfp* fragment was excised from pGEM-T-*pdhS'C-cfp* by *Not*I restriction and subsequently cloned into *Not*I-cut pJQ200-uc1 to generate pDD003.

These pJM056, pJM082 and pDD003 constructions were transformed into *E. coli* strain S17-1, and introduced into *B. abortus* 544 Nal^R strain by conjugation. Transformants that integrated a

plasmid into their chromosome were selected on medium supplied with gentamycin. In order to allow excision, positive clones were cultivated in 2YT without gentamycin for more than 10 generations and plated onto solid medium containing 5% sucrose because *sacB* gene carried on the pJQ200-uc1 vector (5) confers sucrose sensitivity to gram-negative bacteria hence allowing to apply counterselection for allelic replacement. Gentamycin-sensitive but sucrose-resistant colonies were isolated and gene replacement was confirmed by PCR.

Synthetic lethality of fumA and fumC deletions

Many unsuccessful attempts to obtain a Δ*fumA*Δ*fumC* double deletion strain from the XDB1160 strain prompted us to investigate the possible synthetic lethality of these two mutations. We attempted to delete the *fumC* gene in the XDB1160 strain in which we previously introduced the low copy vector pMR10cat (negative control) or pMR10cat carrying a rescuing fumarase CDS. As expected, from 46 clones, none presented the double deletion profile by PCR when pMR10cat was used. In contrast, the same experiments performed with the *fumC-yfp* (pJM063) or *fumA-yfp* (pJM043) rescue copies respectively showed that 11% (=5/46) and 26% (=12/46) of clones tested presented the Δ*fumC* profile by PCR.

Construction of fluorescence and expression destination vectors

Lambda Red technique (3, 4) was used to generate pMR-*nat*R (C. Van der Henst, unpublished data), pJM080 and pJM095 from pMR10 (Mohr and Roberts, unpublished data), pJM063 and pJM043 respectively, by replacing the kanamycin resistance cassette by nat^R, a gene that confers nourseothricine resistance. The nat^R gene was amplified from pFA6-y*fp*-*nat*MX6 (22) with Nourseo-red-up and Nourseo-red-down primers and the resulting amplicon was used for the Lambda Red-based technique, with the MG1655 miniλtet *E. coli* strain.

The vector that allows mCherry N-terminal fusions (mCherry-protein) was constructed as follows : the *mcherry* coding sequence (without its stop codon) was amplified by PCR from pRSET-B-*mcherry* plasmid (19) with the *mcherry*-N-up and *mcherry*-N-down primers and ligated into pGemT-Easy (Promega) to generate pGEM-T-*mcherry*_N. The *mcherry*_N fragment was excised from pGEM-T-*mcherry*_N by *Bam*HI/*Eco*RV double restriction and subsequently cloned into *Bam*HI/*Eco*RV-cut pKSoriT (pBluescript II KS vector from Stratagene in which RP4 *oriT* was inserted in order to make this vector mobilizable) to generate pKSoriT-*mcherry*_N. The so-called rfA cassette (Invitrogen), containing *ccdB* and *cat* genes, was recovered from the pSK-A vector (23) on a 1.7 kb *Eco*RV fragment and subcloned in the same orientation as *mcherry*_N fragment at the *Eco*RV site of pKSoriT-*mcherry*_N to give pKSoriT-*mcherry*_N-K7GWA. Finally the *mcherry*_N-K7GWA fragment was excised from pKSoriT-*mcherry*_N-K7GWA by *Xho*I/*Sac*I double restriction and subsequently inserted into *Xho*I/*Sac*I-cut pMR-*nat*R to generate pCVDH004. Construction and amplification of these Gateway™ destination vectors was performed in the *E. coli* DB3.1 strain (Invitrogen Life-Technologies), that is resistant to *ccdB* toxicity. The Gateway™ recombinational cloning technology (15) was used to insert the CDS of interest into the "destination vectors". BP and LR cloning reactions were performed as recommended by the manufacturer (Invitrogen Life-Technologies).

The vectors that allow mCherry C-terminal fusions (protein-mCherry) were constructed as follows : the *mcherry* coding sequence (without its initial ATG) was amplified by PCR from pRSET-B-*mcherry* (19) with the *mcherry*-C-up and *mcherry*-C-down primers and inserted into pGemT-Easy (Promega) to generate pGEM-T-*mcherry*_C. The *mcherry*_C fragment was excised from pGEM-T-*mcherry*_C by *Eco*RV/*Sal*I double restriction and subsequently cloned into *Eco*RV/*Sal*I-cut pKSoriT to generate pKSoriT-*mcherry*_C. The so-called rfB cassette (Invitrogen) was recovered from the pSK-B vector (23) on a 1.7 kb *Eco*RV fragment and subcloned in the same orientation as *mcherry*_C fragment at the *Eco*RV site of pKSoriT-*mcherry*_C to give pKSoriT-*mcherry*_C-K7GWB. On one hand, the *mcherry*_C-K7GWB fragment was excised from pKSoriT-*mcherry*_C-K7GWB by *Xho*I/*Sac*I double restriction and subsequently ligated into *Xho*I/*Sac*I-cut pMR-*nat*R to generate pCVDH003. On the other hand,

the *kan*R gene was excised from pUC4K (Pharmacia) by *Sal*I digestion and subsequently inserted in the same orientation than *mcherry*_C fragment at the unique *Xho*I site of pKSoriT-*mcherry*_C-K7GWB to generate pCVDH005. Construction and amplification of these Gateway™ destination vectors was performed in the *E. coli* DB3.1 strain (Invitrogen Life-Technologies).
All other plasmids used in this study (Table S1) were constructed by using the Gateway™ technique (Invitrogen). Since *B. abortus* and *B. melitensis* are identical concerning *fumC* and *fumA* genes, entry clones were recovered from the *B. melitensis* ORFeome version 1.1 (7) and checked by sequencing. The pJM109 and pJM110 plasmids were constructed as follows : the *fumC* coding sequences (CDS) were amplified by PCR from *C. crescentus* CB15N or *S. meliloti* 1021 genomic DNA respectively with Gateway™ primers $_{cc}$*fumC-att*B1 and $_{cc}$*fumC-att*B2 (for $_{cc}$*fumC*); $_{sm}$*fumC-att*B1 and $_{sm}$*fumC-att*B2 (for $_{sm}$*fumC*) (Invitrogen Life-Technologies), and cloned in the entry vector pDONR201 as previously described (7).
For plasmids used in the yeast two-hybrid (Y2H) assay, the so-called BD-X and AD-Y constructs are expressed from the bait plasmid pVV212 (23) as C-terminal fusions to Gal4p$_{1-147}$ (BD) and from the prey plasmid pVV213 (23) as C-terminal fusions to Gal4p$_{768-881}$ (AD), respectively. These pVV212 and pVV213 "destination vectors" are pGBT9 (1) and pACT2 (11) derivatives, respectively, compatible with the Gateway™ recombinational cloning technology (25).

Yeast Two-Hybrid Assay and screening of the *B. melitensis* ORFeome
Growth media and yeast genetic techniques have been described previously (20). YPD was used as a rich medium. SD-W and SD-L are respectively tryptophan and leucin omission in synthetic dextrose (SD) media and were used to select MaV103 and MaV203 yeast strains transformed with recombinant pVV212 and pVV213 plasmids, respectively. SD-LW medium lacking both leucin and tryptophan was used to select diploids. SD-HLW + 20 mM 3-AT lacking histidine, leucine and tryptophane and containing 20 mM of 3-amino-triazole (3AT, Sigma) and SD-ULW medium lacking uracil, leucin and tryptophan were used as selective media to detect physical interactions.
The yeast two-hybrid experiments were performed as reported previously (14). BD-X (for which X corresponds to either a single protein, a pool of proteins or no protein) constructs were transformed into MaV103 yeast strain. Transformants were grown at 30°C for three days on SD-W plates. A pool of transformants of each construct (or of each pool of constructs in the case of Y2H screen) was resuspended in 100 µl of SD-W liquid medium and cells were grown overnight at 30°C.
AD-Y (for which Y corresponds to either a single protein or no protein) constructs were transformed into MaV203 yeast strain. Transformants were grown at 30°C for three days on SD-L plates. For each construct, a pool of transformants was resuspended in 100 µl of SD-L liquid medium and cells were grown overnight at 30°C.
The following mating protocol was then used to combine AD-Y fusions with BD-X constructs. The SD-L cultures containing the AD-Y fusions were spotted onto YPD plate and the SD-W cultures containing the BD-X fusions were replica-plated on the same YPD plate. The YPD plate was incubated overnight at 30°C to allow mating to occur. On the next day, the YPD plate was replica-plated onto a SD-LW medium that was incubated at 30°C for one to two days to allow growth of the diploids. To assay expression of both *HIS3*, *URA3* and *lacZ* reporter genes, the diploids were picked and resuspended in a SD-LW liquid medium, grown overnight at 30°C and finally spotted onto SD-HLW (without histidine, leucine and tryptophane) + 20 mM 3-AT, SD-ULW (without uracil, leucine and tryptophane) or YPD plates covered with a phosphocellulose membrane, respectively. The two formers were incubated at 30°C and growth was monitored after 3-5 days. The latter was incubated at 30°C for one day and tested for β-galactosidase production (26).

For the screening of the *B. melitensis* ORFeome with PdhS, *pdhS* coding sequence was fused to BD coding sequence in the pRH412 plasmid. This fusion is suitable for the Y2H screen since no autoactivation was detected for BD-PdhS (data not shown). On the other hand, the 3091 entry clones available in the *Brucella* ORFeome resource were organized into 70 pools of 46 or 48 entry clones and pooled ORFs were fused to the Gal4p activating domain (AD). Precautions were taken to maintain the representativeness of each entry clone in the 70 pools. The screen was performed in two steps. Candidate clones were first selected using the *HIS3* reporter gene and interactions were next validated using *lacZ* and *URA3* reporter genes.

Confirmation of PdhS-FumC interaction by coexpression of *pdhS-cfp* and *fumC-yfp* in *C. crescentus*

In *C. crescentus*, *B. abortus* PdhS-CFP mainly localized to a pole while $_{ba}$FumC was scattered throughout the cytoplasm. To validate FumC recruitment by PdhS, we predicted that if $_{ba}$FumC interacts with PdhS, a FumC-YFP fusion would be recruited at the same PdhS-CFP localization in *C. crescentus*. In order to test this hypothesis by heterologously reconstructing FumC recruitment by PdhS-FumC in *C. crescentus*, we first designed XDB1166, a *C. crescentus* strain expressing a *pdhS-cfp* fusion from the chromosomal inducible *xylX* promoter (P_{xylX}, amplified using P_{xylX}up and P_{xylX}down primers). As expected, when XDB1166 was grown in the presence of glucose, no PdhS-CFP foci were detected. After 5 hours of xylose induction, PdhS-CFP was found at one pole and sometimes at a mid-cell position (Figure 1B). The low copy plasmid pJM080 carrying a *$_{ba}$fumC-yfp* fusion was transformed in the XDB1166 strain, and the resulting strain was grown in the presence of glucose or xylose. In the presence of glucose, PdhS-CFP was not detected by western blot analysis (data not shown) and FumC-YFP was found dispersed throughout the cytoplasm (Figure 1B). Upon the addition of xylose, PdhS-CFP was produced (data not shown) and targeted to a discrete position mid-cell or at one pole (Figure 1B). Strikingly, FumC-YFP formed foci that systematically colocalized with PdhS-CFP. Similar results were obtained with a strain (XDB1167) in which *pdhS'N-cfp* fusion was expressed under P_{xylX} control (data not shown). These data strongly support a model in which PdhS is able to recruit $_{ba}$FumC through its N-terminal domain.

To rule out that PdhS-CFP production induces non-specific recruitment of proteins at particular subcellular locations, the same experiment was performed with the *fumA-yfp* fusion (pJM095) instead of *fumC-yfp*, considering that FumA-YFP would not be recruited by PdhS-CFP and would be diffusely localized in *C. crescentus*. While PdhS-CFP formed foci following xylose induction, FumA-YFP retained its dispersed localization pattern whether the medium was supplied with xylose or not (Figure 1B).

Fumarase activity assays

We overproduced and purified a soluble hexahistidine-tagged *B. abortus* FumC (His_6-FumC) in *E. coli* to test its fumarase activity (for technical details, see below). His_6-FumC exhibited fumarase-specific activity at 37 ± 1 U ($\mu M.min^{-1}.mg^{-1}$), which demonstrated that FumC is indeed a fumarase. Since His-188 is predicted to be part of the active site, we generated and purified a soluble H188N variant (replacement of His-188 by Asn) that did not display any detectable activity (data not shown). FumA also showed fumarase activity since it was able to restore this enzymatic activity in a *E. coli* strain in which all three fumarase genes, *fumA*, *fumB* and *fumC*, were deleted (see below).

Fumarase activity was measured spectrophotometrically at 240 nm at room temperature (22°C) (16). 2.9 ml of L-malate (50 mM) prepared in a potassium phosphate buffer (100 mM NaH_2PO_4, pH 7.6) were transferred to a quartz microcuvette with a 1 cm light path. The reaction was initiated by adding an adequate volume of supernatant (in order to have a reaction rate between 0 and 1 OD unit min^{-1}) and followed for 2 min. Fumarase activity was then compared to protein

concentration to calculate the specific fumarase activity. Protein concentration in the supernatants was determined using the standard Bradford method and calibration was carried out with a range of bovine serum albumin concentration (2). One unit of specific fumarase activity is the amount of L-malate (in μM) converted into fumarate per min and per mg of protein.

The His_6-FumC protein was produced by cloning *fumC* CDS in the pET15b-Gateway vector, using the pJM033 plasmid as the substrate for the recombinational cloning to give the pCVDH010 plasmid. The pET15b-Gateway vector was previously constructed by the insertion of "reading frame C.1" (rfC.1) Gateway cassette (Invitrogen) into the filled in *Bam*HI restriction site of pET15b plasmid (Novagen; V. Van Mullem and B. Van Driessche, unpublished data). The overexpression plasmid was transformed into the BL21(DE3) strain. The strain was grown in 200 ml of LB with 50 $\mu g\ ml^{-1}$ ampicillin. When the culture reached an OD^{600} of 0.6, 1 mM IPTG was added and the culture was resumed for 3 hours. After cooling for 10 min on ice, the cells were collected by centrifugation (15 min at 2680 g), and resuspended in a lysis buffer, 50 mM NaH_2PO_4, pH 7.3, with a complete mix of antiprotease agents for *E. coli*, without EDTA (Sigma). The suspension was sonicated on ice (6 times 30 s) and the lysis mix was centrifuged for 25 min at 32,800 g. The supernatant (soluble fraction) was purified on a Ni-NTA column (Qiagen), following the manufacturer's instructions. The His_6-FumC protein eluted as a single band, which was assayed for specific fumarase activity, as described above.

We constructed a triple null mutant (Δ*fumA*, Δ*fumB* and Δ*fumC*) strain of *E. coli* (XDB1130) in which fumarase activity was below the detection level ($<10^{-3}$ U). The XDB1130 strain transformed with a pMR10cat low-copy vector carrying the *fumA* CDS (pJM083) displayed a specific activity of 8.9 ± 0.6 U in the sonicated cell extracts, while the specific activity was 5.1 ± 0.6 U for the positive control wild-type strain (MG1655) transformed by the pMR10cat vector. To perform these activity assays, strains were grown in 150 ml of medium at a starting OD^{600} of 0.03. At OD^{600} 0.05, IPTG (1 mM) was added in order to derepress expression of the gene under P_{lac} control on the pMR10cat vector derivatives. When OD^{600} reached 1, the culture was cooled for 20 min on ice, the cells were harvested (10 min at 8200 g) and washed twice in a 0.2% KCl solution to be finally resuspended in 2 ml of buffer containing Tris-HCl (275 mM) at pH 7.8, glycerol (10% v/v), $MgCl_2$ (11 mM) and DTT (1 mM). The cells were disrupted by sonication using an ultrasonic disruptor (4 cycles of 30 s). Cell debris were removed by centrifugation (7000 rpm for 10 min at 4°C), and the supernatants were used for the enzymatic assays.

Western blot

For every fluorescent observation reported in this study, we carried out western blot analyses with antibodies that recognize either both YFP and CFP or mCherry. The results allowed us to rule out the possibility that the absence of foci could result from protein degradation or a deficiency in fusion protein production (data not shown).

The western blot analyses were carried out as described previously (6) with monoclonal antibodies against GFP (JL-8, Clontech) or mCherry (anti-DsRed, Clontech) that were used at dilutions of 1/2000 or 1/1000 respectively to check the stability of the translational fusions to CFP and YFP or mCherry.

Microscopy

All strains were analysed during the exponential growth phase. For the fluorescence imaging, cell populations of *B. abortus*, *C. crescentus* or *S. meliloti* strains were immobilized on a microscope slide that was layered with a pad of 1% agarose containing PBS (17). These slides were placed on a microscope stage at room temperature (approximately 22°C). The samples were observed on a Nikon E1000 microscope through a 100X differential interference contrast (DIC, Normarski) objective with a Hamamatsu Orca-ER LCD camera. Images acquisition and processing were performed with Simple PCI (Hamamatsu) or NIS element (Nikon) software. For each protein localization described in this study, the experiments were performed at least twice on three independent cultures. For each observation under microscope, three or more fields were selected randomly at distant parts of the agarose pad.

Bibliography

1. **Bartel, P., C. T. Chien, R. Sternglanz, and S. Fields.** 1993. Elimination of false positives that arise in using the two-hybrid system. Biotechniques **14:**920-4.
2. **Bradford, M. M.** 1976. A rapid and sensitive method for the quantitation of microgram quantities of protein utilizing the principle of protein-dye binding. Anal. Biochem. **72:**248-54.
3. **Court, D. L., S. Swaminathan, D. Yu, H. Wilson, T. Baker, M. Bubunenko, J. Sawitzke, and S. K. Sharan.** 2003. Mini-lambda: a tractable system for chromosome and BAC engineering. Gene **315:**63-9.
4. **Datsenko, K. A., and B. L. Wanner.** 2000. One-step inactivation of chromosomal genes in Escherichia coli K-12 using PCR products. Proc Natl Acad Sci U S A **97:**6640-5.
5. **Donnenberg, M. S., and J. B. Kaper.** 1991. Construction of an eae deletion mutant of enteropathogenic Escherichia coli by using a positive-selection suicide vector. Infect Immun **59:**4310-7.
6. **Dozot, M., R. A. Boigegrain, R. M. Delrue, R. Hallez, S. Ouahrani-Bettache, I. Danese, J. J. Letesson, X. De Bolle, and S. Kohler.** 2006. The stringent response mediator Rsh is required for *Brucella melitensis* and *Brucella suis* virulence, and for expression of the type IV secretion system VirB. Cell. Microbiol. **8:**1791-802.
7. **Dricot, A., J. F. Rual, P. Lamesch, N. Bertin, D. Dupuy, T. Hao, C. Lambert, R. Hallez, J. M. Delroisse, J. Vandenhaute, I. Lopez-Goni, I. Moriyon, J. M. Garcia-Lobo, F. J. Sangari, A. P. Macmillan, S. J. Cutler, A. M. Whatmore, S. Bozak, R. Sequerra, L. Doucette-Stamm, M. Vidal, D. E. Hill, J. J. Letesson, and X. De Bolle.** 2004. Generation of the *Brucella melitensis* ORFeome version 1.1. Genome Res. **14:**2201-6.
8. **Ely, B.** 1991. Genetics of *Caulobacter crescentus*. Methods Enzymol. **204:**372-84.
9. **Evinger, M., and N. Agabian.** 1977. Envelope-associated nucleoid from Caulobacter crescentus stalked and swarmer cells. J Bacteriol **132:**294-301.
10. **Finan, T. M., B. Kunkel, G. F. De Vos, and E. R. Signer.** 1986. Second symbiotic megaplasmid in *Rhizobium meliloti* carrying exopolysaccharide and thiamine synthesis genes. J. Bacteriol. **167:**66-72.
11. **Fromont-Racine, M., J. C. Rain, and P. Legrain.** 1997. Toward a functional analysis of the yeast genome through exhaustive two-hybrid screens. Nat Genet **16:**277-82.
12. **Glazebrook, J., and G. C. Walker.** 1991. Genetic techniques in *Rhizobium meliloti*. Methods Enzymol. **204:**398-418.

13. **Hallez, R., J. J. Letesson, J. Vandenhaute, and X. De Bolle.** 2007. Gateway-based destination vectors for functional analyses of bacterial ORFeomes: application to the Min system in Brucella abortus. Appl Environ Microbiol **73:**1375-9.
14. **Hallez, R., J. Mignolet, V. Van Mullem, M. Wery, J. Vandenhaute, J. J. Letesson, C. Jacobs-Wagner, and X. De Bolle.** 2007. The asymmetric distribution of the essential histidine kinase PdhS indicates a differentiation event in *Brucella abortus*. EMBO J. **26:**1444-55.
15. **Hartley, J. L., G. F. Temple, and M. A. Brasch.** 2000. DNA cloning using in vitro site-specific recombination. Genome Res **10:**1788-95.
16. **Hill, R. L., and R. A. Bradshaw.** 1969. Fumarase. Methods in Enzymology **13:**91-99.
17. **Jacobs, C., I. J. Domian, J. R. Maddock, and L. Shapiro.** 1999. Cell cycle-dependent polar localization of an essential bacterial histidine kinase that controls DNA replication and cell division. Cell **97:**111-20.
18. **Meade, H. M., S. R. Long, G. B. Ruvkun, S. E. Brown, and F. M. Ausubel.** 1982. Physical and genetic characterization of symbiotic and auxotrophic mutants of Rhizobium meliloti induced by transposon Tn5 mutagenesis. J Bacteriol **149:**114-22.
19. **Shaner, N. C., R. E. Campbell, P. A. Steinbach, B. N. Giepmans, A. E. Palmer, and R. Y. Tsien.** 2004. Improved monomeric red, orange and yellow fluorescent proteins derived from Discosoma sp. red fluorescent protein. Nat Biotechnol **22:**1567-72.
20. **Sherman, F.** 1991. Getting started with yeast. Methods Enzymol. **194:**3-21.
21. **Simon, R., Priefer, U., and Pühler, A.** 1983. A broad host range mobilisation system for in vivo genetic engineering: transposon mutagenesis in gram negative bacteria. Biotechnology **10:**783-791.
22. **Van Driessche, B., L. Tafforeau, P. Hentges, A. M. Carr, and J. Vandenhaute.** 2005. Additional vectors for PCR-based gene tagging in Saccharomyces cerevisiae and Schizosaccharomyces pombe using nourseothricin resistance. Yeast **22:**1061-8.
23. **Van Mullem, V., M. Wery, X. De Bolle, and J. Vandenhaute.** 2003. Construction of a set of Saccharomyces cerevisiae vectors designed for recombinational cloning. Yeast **20:**739-46.
24. **Vidal, M., R. K. Brachmann, A. Fattaey, E. Harlow, and J. D. Boeke.** 1996. Reverse two-hybrid and one-hybrid systems to detect dissociation of protein-protein and DNA-protein interactions. Proc Natl Acad Sci U S A **93:**10315-20.
25. **Walhout, A. J., G. F. Temple, M. A. Brasch, J. L. Hartley, M. A. Lorson, S. van den Heuvel, and M. Vidal.** 2000. GATEWAY recombinational cloning: application to the cloning of large numbers of open reading frames or ORFeomes. Methods Enzymol **328:**575-92.
26. **Walhout, A. J., and M. Vidal.** 2001. High-throughput yeast two-hybrid assays for large-scale protein interaction mapping. Methods **24:**297-306.
27. **Xiao, H., M. Kalman, K. Ikehara, S. Zemel, G. Glaser, and M. Cashel.** 1991. Residual guanosine 3',5'-bispyrophosphate synthetic activity of relA null mutants can be eliminated by spoT null mutations. J Biol Chem **266:**5980-90.

Supplementary Tables

Table S1. Strains and Plasmids

Strain	Relevant Genotype or Description	Reference or Source
B. abortus		
544 Nal^R	nalidixic acid-resistant B. *abortus* 544	J-M. Verger
XDB1150	*B. abortus* 544 *fumC::fumC-yfp*	This study
XDB1151	*B. abortus* 544 *fumC::fumC-cfp*	This study
XDB1152	*B. abortus* 544 *fumC::fumC-mcherry*	This study
XDB1153	*B. abortus* 544 *fumA::fumA-yfp*	This study
XDB1155	*B. abortus* 544 *pdhS-cfp*	This study
XDB1156	*B. abortus* 544 *pdhS-cfp/fumC::fumC-yfp*	This study
XDB1157	*B. abortus* 544 Δ*fumC*	This study
XDB1158	*B. abortus* 544 Δ*fumC/pdhS-cfp*	This study
XDB1159	*B. abortus* 544 Δ*fumC/fumA::fumA-yfp*	This study
XDB1160	*B. abortus* 544 Δ*fumA*	This study
XDB1161	*B. abortus* 544 Δ*fumA/fumC::fumC-yfp*	This study
C. crescentus		
CB15N	Synchronizable variant strain of CB15	(9)
XDB1165	CB15N $_{cc}$*fumC::* $_{cc}$*fumC-yfp*	This study
XDB1166	CB15N P_{xylX}::P_{xylX}-*pdhS-cfp*	This study
XDB1167	CB15N P_{xylX}::P_{xylX}-*pdhS'N-cfp*	This study
S. meliloti		
1021	wild type strain	(18)
E. coli		
DH10B	Cloning strain	Invitrogen Life-Technologies
DB3.1	*ccdB* resistant cloning strain	Invitrogen Life-Technologies
BL21(DE3)	Host strain for protein overproduction	Novagen
S17-1	RP4-2, Tc::Mu,Km-Tn7, for plasmid mobilization	(21)
DH5α	Donor strain in triparental mating	Bethesda Research Laboratories
MT616	Helper strain in triparental mating	(10)
MG1655	F^-, λ^-variant strain of *E. coli* K12	(27)
MG1655 miniλtet	tet resistant, integrated mini phage λ strain for λred recombination	(3)
XDB1130	MG1655 Δ*fumA* Δ*fumB* Δ*fumC*	This study
Saccharomyces cerevisiae (yeast)		
MaV103	*MATa leu2-3, 112 trp-901 his3Δ200 ade2-1 gal4Δ gal80Δ SPAL10::URA3 GAL1::lacZ GAL1::HIS3-@LYS2 can1^R cyh2^R*	(24)
MaV203	*MATα leu2-3112 trp-901 his3Δ200 ade2-1 gal4Δ gal80Δ SPAL10::URA3 GAL1::lacZ GAL1::HIS3-@LYS2 can1^R cyh2^R*	(24)

Plasmid	Relevant Genotype or Description	Reference or Source
pJM056	pJQ200-uc1 carrying Δ*fumC*	This study
pJM082	pJQ200-uc1 carrying Δ*fumA*	This study
pDD003	pJQ200-uc1 carrying *pdhS'C-cfp*	This study
pJM033	pDONR201 carrying *fumC*	This study
pJM042	pDONR201 carrying *fumA*	This study
pJM109	pDONR201 carrying $_{cc}$*fumC*	This study
pJM110	pDONR201 carrying $_{sm}$*fumC*	This study
pRH402	pDONR201 carrying *pdhS'N*	(14)
pRH403	pDONR201 carrying *pdhS'C*	(14)
pMR10cat	Broad host range low copy vector	C. Mohr and R. Roberts
pET15b-GW	Gateway-compatible pET15b (Novagen)	V. Van Mullem, unpublished
pCVDH010	pET15b-GW carrying *fumC*	This study
pRH005	Gateway-compatible YFP low copy vector	(13)
pJM063	pRH005 carrying *fumC-yfp*	This study
pJM043	pRH005 carrying *fumA-yfp*	This study
pJM105	pRH005 carrying $_{cc}$*fumC-yfp*	This study
pJM106	pRH005 carrying $_{sm}$*fumC-yfp*	This study
pJM080	pRH005 nat^R carrying *fumC-yfp*	This study
pJM095	pRH005 nat^R carrying *fumA-yfp*	This study
pCVDH003	Gateway-compatible mCherry low copy vector	This study
pCVDH004	mCherry gateway-compatible low copy vector	This study
pCVDH005	Gateway-compatible mCherry suicide vector	This study
pCVDH008	pCVDH005 carrying *fumC-mcherry*	This study
pRH011	Gateway-compatible YFP suicide vector	(13)
pJM053	pRH011 carrying *fumC-yfp*	This study
pJM044	pRH011 carrying *fumA-yfp*	This study
pJM099	pRH011 carrying $_{cc}$*fumC-yfp*	This study
pRH010	Gateway-compatible CFP suicide vector	(13)
pJM052	pRH010 carrying *fumC-cfp*	This study
pJM074	pRH010 carrying P_{xylX}-*pdhS-cfp*	This study
pJM115	pRH010 carrying P_{xylX} -*pdhS'N-cfp*	This study
pVV212	Gateway-compatible BD_Gal4 vector	(23)
pRH412	pVV212 carrying BD-*pdhS*	(14)
pJM067	pVV212 carrying BD-*fumC*	This study
pJM078	pVV212 carrying BD-*fumA*	This study
pVV213	Gateway-compatible AD_Gal4 vector	(23)
pRH413	pVV213 carrying AD-*pdhS*	(14)
pRH414	pVV213 carrying AD- *pdhS'N*	(14)
pRH123	pVV213 carrying AD *pdhS'C*	(14)

Table S2. Primers used in this study

Name	Sequence 5' to 3'
*fumC*up1	GGGGTACCCCCCTCGGATATTTGTCACGAC
*fumC*up2	TTGGCTGCAGTTGAAGATCTTCGTGGCGGCCATTTCATGTC
*fumC*down1	GAAGATCTTCAACTGCAGCCAAATCGCCCCACAATGAATTGC
*fumC*down2	CGGGATCCCGGGAAGTCCAGAACTGGTGG
*fumA*up1	GGGGTACCCCCATTGGATGCAGGAGCAGC
*fumA*up2	TTGGCTGCAGTTGAAGATCTTCGCTTCTGCCATCGTGGTAC
*fumA*down1	GAAGATCTTCAACTGCAGCCAATTCAACCTGAGTTGACCGC
*fumA*down2	CGGGATCCCGCAGTGCCTGAATGGCATTG
*pdhS-cfp*up1	GCTCGATATGCAGTTCGAGGCG
*pdhS-cfp*up2	TGGAGATATCAGCCAGAACGCG
*pdhS-cfp*down1	GGCTGATATCTCCAATCAGATTG
*pdhS-cfp*down2	GCCGGAACCGCTCTAACTATTTG
*cfp*up	GTGAGCAAGGGCGAGGAGCTG
*cfp*down	TCACTTGTACAGCTCGTCCATGCCG
P_{xylX} up	CGGAGATCTTCGAATTCTCGAACAGGGCCG
P_{xylX} down	CGGAGATCTTCCATATGGTCGTCTCCCCAAA
*pdhS-att*B1	GGGGACAAGTTTGTACAAAAAAGCAGGCTTAATGTCAGGATCATACCCCTTCAT
*pdhS-att*B2	GGGGACCACTTTGTACAAGAAAGCTGGGTAGTCAGCCAGAACGCGGGTT
$_{cc}$*fumC-att*B1	GGGGACAAGTTTGTACAAAAAAGCAGGCTTAATGACCGCCACGCGTATCGA
$_{cc}$*fumC-att*B2	GGGGACCACTTTGTACAAGAAAGCTGGGTAGCCCGGCGAGATCATCTTTTC
$_{sm}$*fumC-att*B1	GGGGACAAGTTTGTACAAAAAAGCAGGCTTAATGACATCGACCCGCACGGA
$_{sm}$*fumC-att*B2	GGGGACCACTTTGTACAAGAAAGCTGGGTAGGCCGGGCCGATCATGGTT
Nourseo-red-up	ACTGTCTGCTTACATAAACAGTAATACAAGGGGTGTTATGGGTACCACTCTTGACGA
Nourseo-red-down	TGCTCTGCCAGTGTTACAACCAATTAACCAATTCTGATTAGGGGCAGGGCATGCTCA
mcherry-N-up	GGATCCATGGTGAGCAAGGGCGAGGA
mcherry-N-down	GATATCCTTGTACAGCTCGTCCATGC
mcherry-C-up	GATATCGTGAGCAAGGGCGAGGAGGA
mcherry-C-down	CTCGAGTTACTTGTACAGCTCGTCCA

Supplementary Figures

Figure S1. Alignment between *B. abortus* FumC and *E. coli* FumC. The alignment was performed with Clustalw server at European Bioinformatics Institute (www.ebi.ac.uk/clustalw/). The two sequences share 58% identities and 71% similarities (using the Blosum scoring matrix). Residues involved in catalysis in the *E. coli* FumC (EcfumC) enzyme are boxed, they are all conserved in *B. abortus* FumC (BafumC). Underlined sections of the alignment correspond to the regions of the proteins involved in the structure of the catalytic site, their sequence is highly conserved in the *B. abortus* FumC. The positions with a star (*) are conserved residues, while similar residues are indicated by dots (: for high similarity). Accession numbers of *B. abortus* and *E. coli* FumC in UniProtKB are Q2YIJ6 and P05042, respectively.

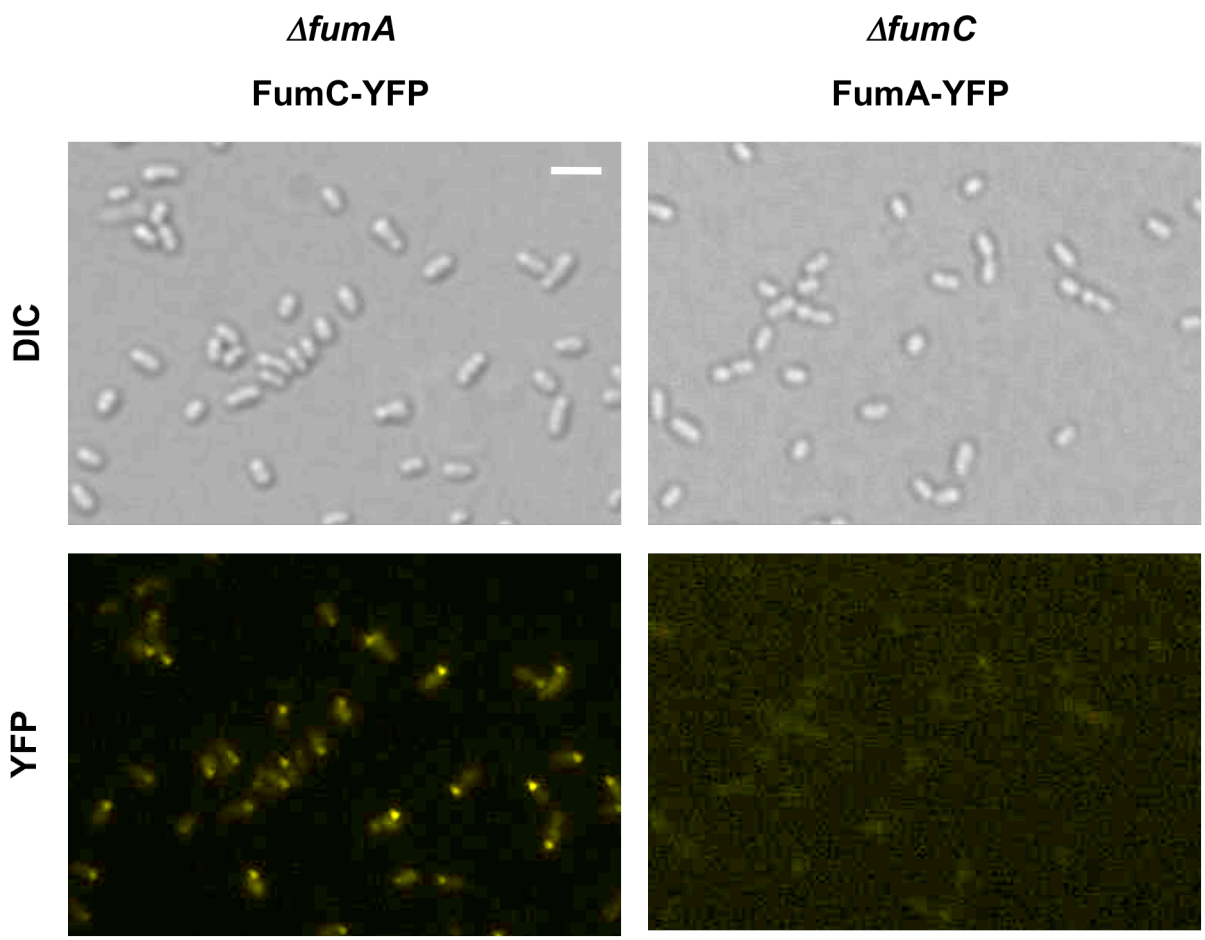

Figure S2. Deletion of one fumarase gene does not modify localization of the other fumarase fused to YFP. In order to test the possible impact of the absence of one fumarase on the localization of the other, the two following experiences were performed. First FumC-YFP has been produced in a Δ*fumA* strain (XDB1161), and second a FumA-YFP fusion was produced in the Δ*fumC* strain (XDB1159). The localization pattern in these two strains is very similar to the wild type control shown in Figure 2.

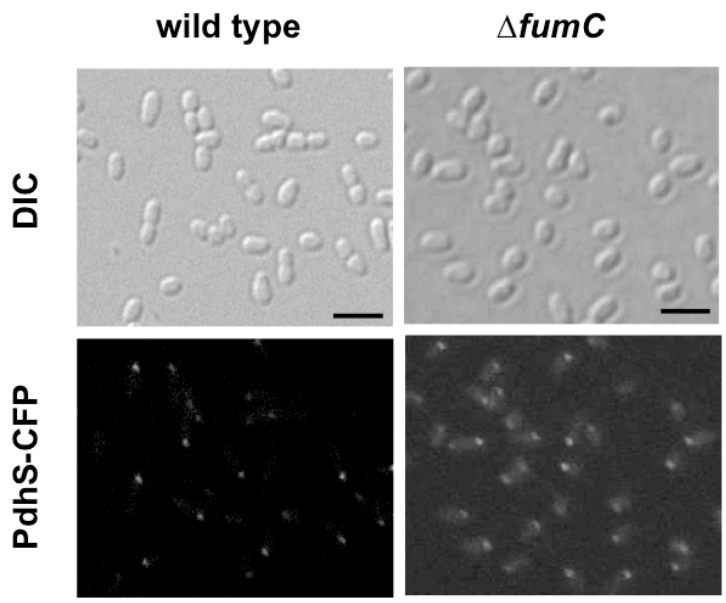

Figure S3. Polar localization of PdhS-CFP in either wild-type or Δ*fumC B. abortus*. Micrographs taken using DIC (Normarski) and CFP characteristic fluorescence are shown for XDB1155, a strain carrying a *pdhS-cfp* fusion at the *pdhS* locus, and for XDB1158, a *fumC* deletant strain carrying a *pdhS-cfp* fusion at the *pdhS* locus. The localization profile of PdhS-CFP is indistinguishable between the two strains. A total of 673 bacteria were examined for the *pdhS-cfp* (XDB1155) strain, while 546 bacteria were screened for the Δ*fumC/pdhS-cfp* (XDB1158) strain. The scale bars represent 2 μm.

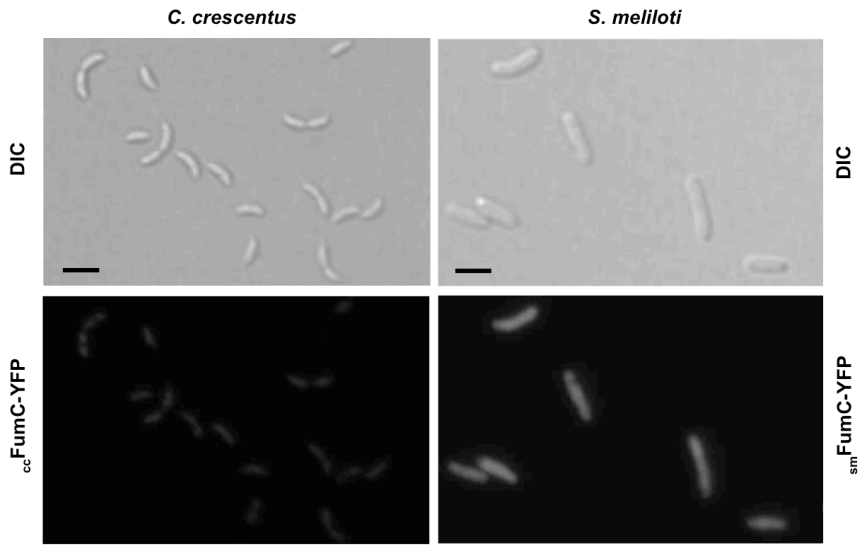

Figure S4. *C. crescentus* and *S. meliloti* FumC-YFP are not polarly localized like *B. abortus* FumC-YFP. The $_{sm}$FumC-YFP was produced from a replicative plasmid and $_{cc}$FumC-YFP from the chromosomal *$_{cc}$fumC* locus (XDB1165 strain), as described in the text. When expressed on a low-copy plasmid under control of the *E. coli lac* promoter, *$_{cc}$fumC-yfp* yielded a localisation pattern typical of overexpression (Figure S5). The bacteria were observed using DIC (Normarski) and characteristic YFP fluorescence. The scale bars represent 2 μm.

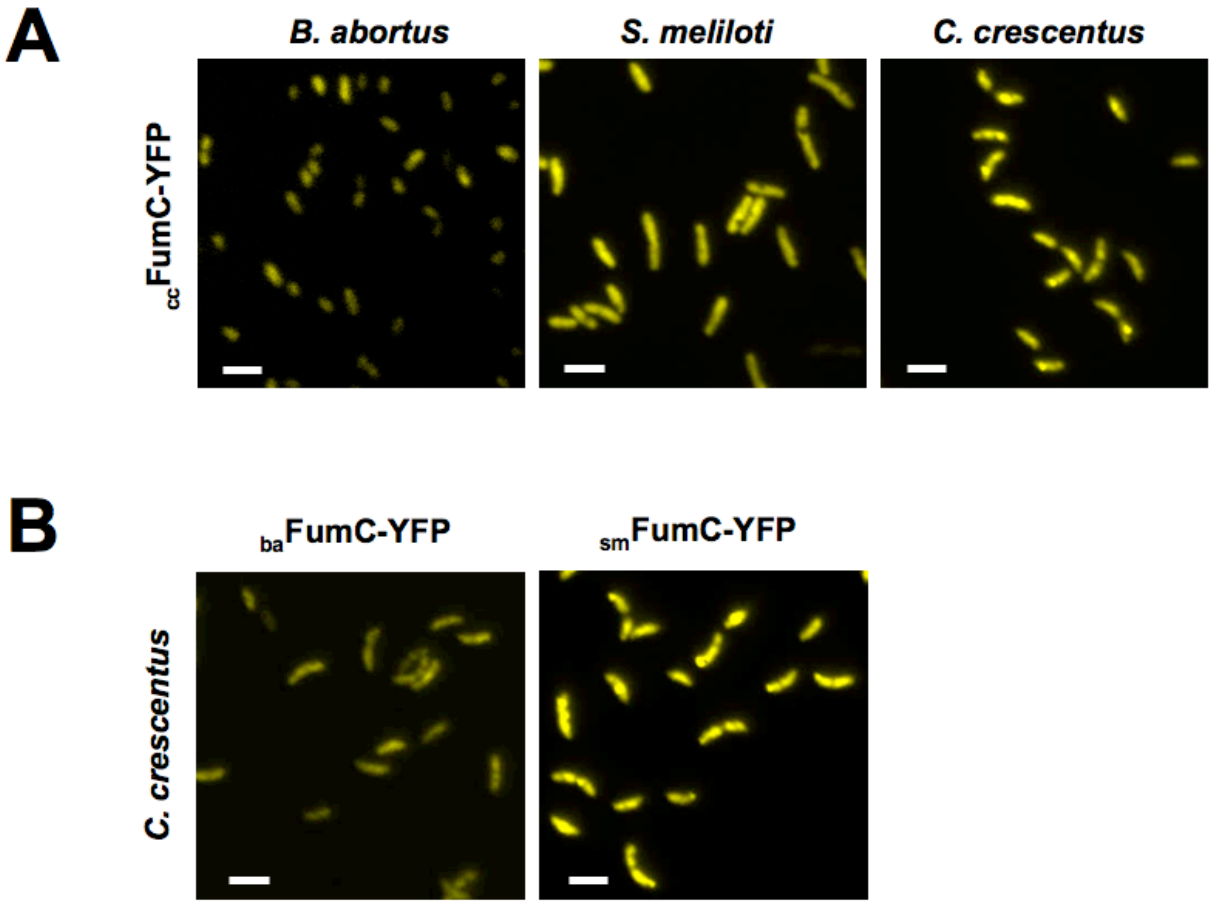

Figure S5. Localization of $_{cc}$FumC in three α-proteobacteria and localization of $_{ba}$FumC and $_{sm}$FumC in *C. crescentus*. (A) The pJM105 plasmid carrying *$_{cc}$fumC-yfp* was introduced in Δ*fumC B. abortus*, *S. meliloti* 1021 and *C. crescentus* CB15N. (B) The *$_{ba}$fumC-yfp* and *$_{sm}$fumC-yfp* were carried by pJM063 and pJM106 respectively. The localization pattern do not ressemble the unipolar labeling shown in Figure 3 for $_{ba}$FumC-YFP in *B. abortus* and *S. meliloti*. The heterogenous localization visible for some strains may be artefacts due to overexpression of the fusions.

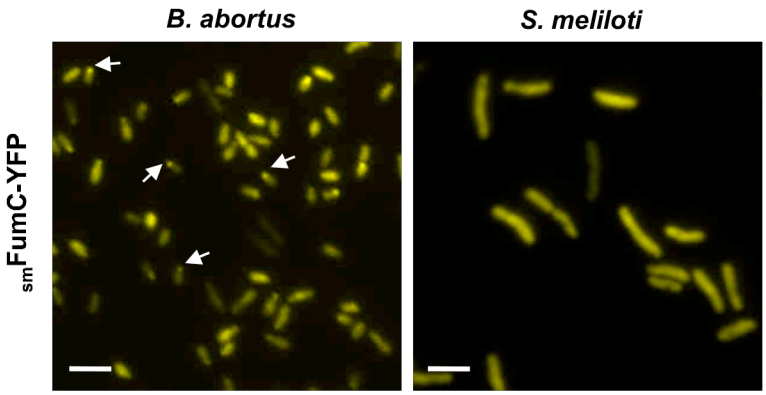

Figure S6. Localization of $_{sm}$FumC in *B. abortus* and *S. meliloti*. FumC-YFP fusion was constructed with the FumC homologs from *S. meliloti*. The localization profile of this fusion was observed in the two species in the exponential growth phase of the culture. Some *B. abortus* cells displaying a polar $_{sm}$FumC-YFP localization are indicated with a white arrow. The scale bars represent 2 μm.

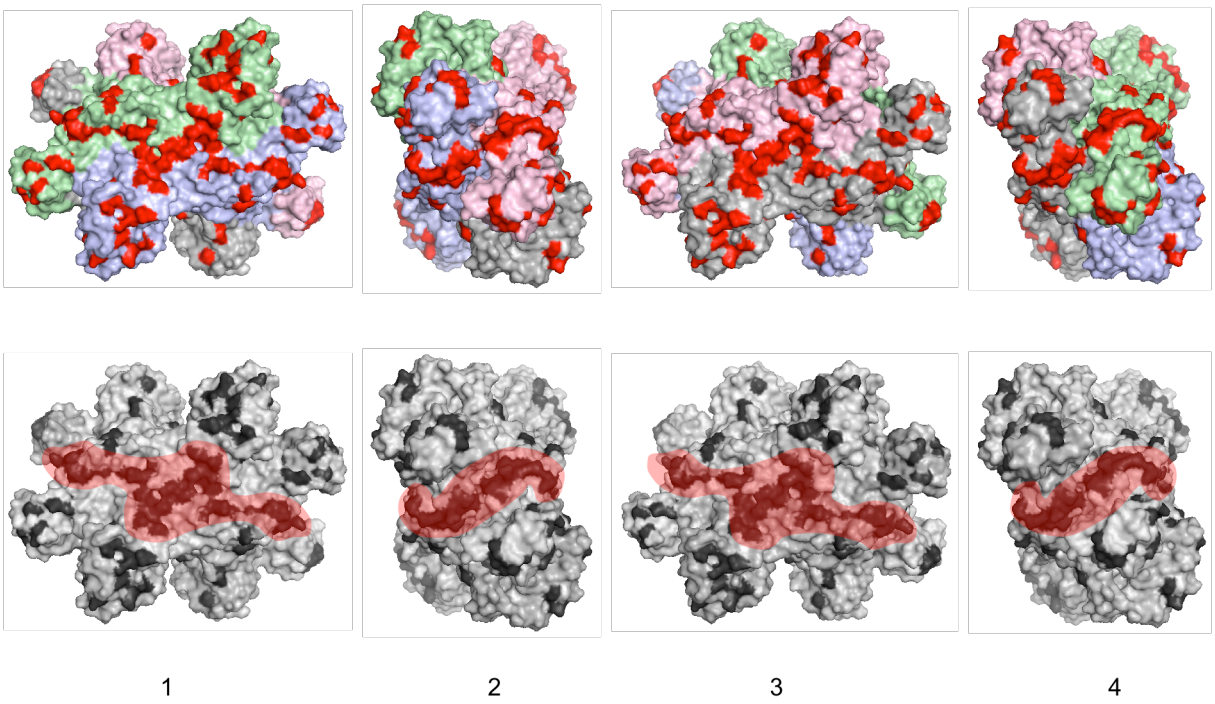

Figure S7. Structural analysis of the substitutions between *B. abortus* and *S. meliloti* FumC homologs. From the alignment of $_{ba}$FumC and $_{sm}$FumC (70% identities), poorly conserved residues (according to the Clustalw program, European Bioinformatics Institute, www.ebi.ac.uk/clustalw/) were reported to the corresponding positions on the tetrameric structure of *E. coli* FumC (1YFE in the Protein Databank). On the top part of the figure, each monomer is shown with a different color (grey, pink, blue and green). The substitutions between *S. meliloti* and *B. abortus* FumC homologs are shown in red. On the bottom part of the figure, the substitutions forming a "belt" around the tetramer are highlighted by a red surface.The four different views (labeled 1 to 4) of the tetramer correspond to successive rotations of 90° around a vertical axis.

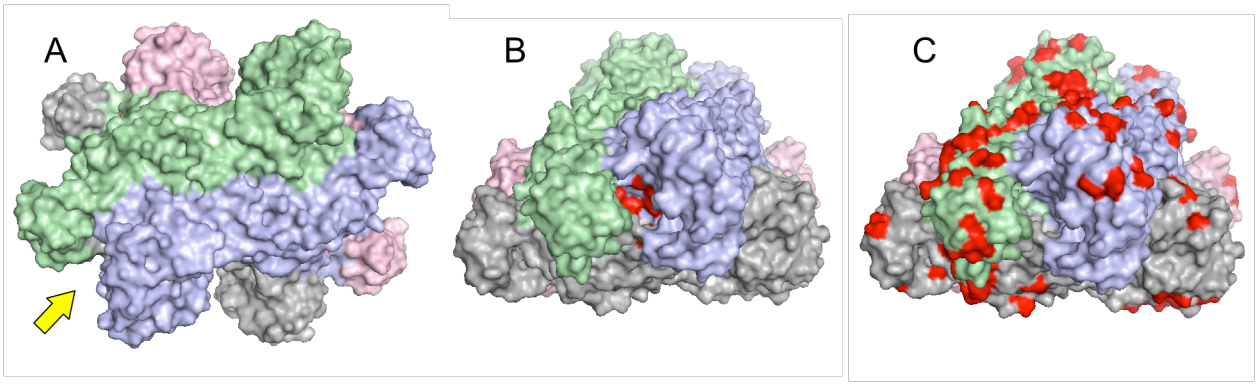

Figure S8. Substitutions between *B. abortus* and *S. meliloti* FumC homologs are not predicted to directly affect catalytic site. (A) The tetrameric *E. coli* FumC structure is represented in the same orientation as in Figure S7, with the same color code for the four subunits. The yellow arrow shows the orientation taken to give part B. None of the catalytic residues are visible in the « A » orientation. (B) Positioning of the catalytic site residues boxed in figure S1, here shown in red. The residues are mostly buried into a deep pocket in the structure. (C) Positioning of the substitutions between *B. abortus* and *S. meliloti* FumC homologs, shown in the same orientation as in part B. These substitutions are not located in the catalytic pocket.